Subunit determination of the conductance of hair-cell mechanotransducer channels

Maryline Beurg[a], Wei Xiong[b], Bo Zhao[b], Ulrich Müller[b], and Robert Fettiplace[a,1]

[a]Department of Neuroscience, University of Wisconsin School of Medicine and Public Health, Madison, WI 53706; and [b]Department of Molecular and Cellular Neuroscience, Dorris Neuroscience Center, The Scripps Research Institute, La Jolla, CA 92037

Cochlear hair cells convert sound stimuli into electrical signals by gating of mechanically sensitive ion channels in their stereociliary (hair) bundle. The molecular identity of this ion channel is still unclear, but its properties are modulated by accessory proteins. Two such proteins are transmembrane channel-like protein isoform 1 (TMC1) and tetraspan membrane protein of hair cell stereocilia (TMHS, also known as lipoma HMGIC fusion partner-like 5, LHFPL5), both thought to be integral components of the mechanotransduction machinery. Here we show that, in mice harboring an *Lhfpl5* null mutation, the unitary conductance of outer hair cell mechanotransducer (MT) channels was reduced relative to wild type, and the tonotopic gradient in conductance, where channels from the cochlear base are nearly twice as conducting as those at the apex, was almost absent. The macroscopic MT current in these mutants was attenuated and the tonotopic gradient in amplitude was also lost, although the current was not completely extinguished. The consequences of *Lhfpl5* mutation mirror those due to *Tmc1* mutation, suggesting a part of the MT-channel conferring a large and tonotopically variable conductance is similarly disrupted in the absence of *Lhfpl5* or *Tmc1*. Immunolabelling demonstrated TMC1 throughout the stereociliary bundles in wild type but not in *Lhfpl5* mutants, implying the channel effect of *Lhfpl5* mutations stems from down-regulation of TMC1. Both LHFPL5 and TMC1 were shown to interact with protocadherin-15, a component of the tip link, which applies force to the MT channel. We propose that titration of the TMC1 content of the MT channel sets the gradient in unitary conductance along the cochlea.

cochlea | mechanotransducer channels | TMC1 | hair cell | LHFPL5

Cochlear hair cells detect sound stimuli by submicron vibrations of their stereociliary (hair) bundles. The stereocilia are arranged in three to four rows, stepped in height and interconnected by extracellular linkages; the most important for transduction are the tip links (1, 2), composed of cadherin-23 and protocadherin-15 (3, 4). During bundle displacements, they transmit force to activate mechanotransducer (MT) ion channels near the insertion of protocadherin-15 at the lower end of the tip link into the stereociliary tip (5, 6). The molecular identity of the pore-forming subunit of the ion channel is still controversial, but there has been a recent proposal that transmembrane channel-like protein isoforms 1 and 2 (TMC1 and TMC2) (7, 8) are possible candidates (9, 10); mutations of these proteins can alter the Ca^{2+} selectivity and single-channel conductance of the MT channels, implying that TMC proteins can influence ion conduction through the pore (10–12). However, in *Tmc1/Tmc2* double mutants, large mechanically sensitive currents can still be evoked and flow through channels similar to native MT channels (13). Thus, an alternate view is that the TMC1 and TMC2 are accessory but not pore-forming subunits of the channel.

Another likely component of the transduction machinery is the tetraspan membrane protein, lipoma HMGIC fusion partner-like 5 (LHFPL5) (14). A variety of evidence suggests that LHFPL5 interacts with both protocadherin-15 and the MT channel. LHFPL5 is localized near the stereociliary tips. Coimmunoprecipitation experiments show that LHFPL5 interacts with the cytoplasmic domain of protocadherin-15, and furthermore, expression of the two proteins is correlated: a deficiency in one leads to down-regulation in the other (14). In *Lhfpl5*$^{-/-}$ mice, the macroscopic MT current is reduced in apical outer hair cells (OHCs), indicating LHFPL5 can, like TMC1, modulate channel properties. The present experiments examine the interactions between LHFPL5 and TMC1 and show that the effects of *Lhfpl5* knockout are largely due to reduced expression of TMC1 in the hair bundle. Evidence is also obtained indicating that both proteins interact with the MT channel and also with protocadherin-15, the protein constituent at the lower end of the extracellular tip link, which dispenses force to the channel.

Results

MT Currents in OHCs of *Lhfpl5* Mutants. In wild-type or *Lhfpl5* heterozygotes, sinusoidal motion of the hair bundle about its resting position evoked a saturated MT current with a peak-to-peak amplitude that increased from cochlear apex to base (Fig. 1 *A* and *C*) as reported for other rodents (15, 16). The current was asymmetric with the principal inward component flowing at the −84 mV holding potential through MT channels opened by displacements of the hair bundle toward its taller edge, as is normally observed (17). By contrast, in *Lhfpl5*$^{-/-}$, not only was there a reduction in the current amplitude for the normal polarity of bundle displacement (14), but often there was a two-harmonic response with the component of current for negative

Significance

Cochlear hair cells are sensory receptors of the inner ear that detect sound via opening of mechanically sensitive transduction channels at the tips of the eponymous hairs. The conductance of the channel increases two-fold along the cochlea, but neither its molecular structure nor mechanism of tonotopic variation is known. We show that when either of two deafness-linked proteins, transmembrane channel-like protein isoform 1 (TMC1) and tetraspan membrane protein of hair cell stereocilia (TMHS, also known as lipoma HMGIC fusion partner-like 5, LHFPL5) is knocked out, the conductance variation is lost. Furthermore, the effect of LHFPL5 is attributable to down-regulation of TMC1, suggesting that titrating the TMC1 content of the channel modulates its conductance. Evidence indicates that both proteins interact with the mechanotransduction channel and also with protocadherin-15, a component of the extracellular tip link that applies force to the channel.

Fig. 1. MT currents in OHCs of mouse *Lhfpl5* mutants. (*A*) MT currents evoked by sinusoidal fluid-jet stimuli in OHCs from the cochlear apex (*d* = 0.2; *Left*) and cochlear base (*d* = 0.75; *Right*) in *Lhfpl5*$^{+/-}$ heterozygotes. (*B*) MT currents were evoked by sinusoidal fluid-jet stimuli in OHCs from the cochlear apex (*Left*) and cochlear base (*Right*) in *Lhfpl5*$^{-/-}$. The two-harmonic response included a reduced amplitude normal response and also a larger reverse-polarity current produced by deflections of bundle away from its taller edge. The driving voltage to the fluid-jet piezoelectric disk, V_{PIEZO}, is shown at the top and was calibrated to give hair bundle motion with amplitude of ~130 nm in *Lhfpl5* heterozygotes and 80 nm in *Lhfpl5* knockouts. (*C*) Peak MT current for the heterozygote, *Lhfpl5*$^{+/-}$ (open circles) and for the knockout *Lhfpl5*$^{-/-}$ (filled circles) is plotted against *d*, the cochlear location. Filled circles are for the conventional stimulus–polarity response. Each point is the mean ± 1 SEM, with numbers of cells, each from a different animal, indicated next to the points. Note the mean current increases toward the high-frequency base for the heterozygote, but not for the knockout. (*D*) Peak reverse-polarity currents (mean ± 1 SD) shown for apex and base as in *C*. The recordings at the base were from P2–P4 mice and those at the apex were from P4–P6 mice, the difference reflecting the two-day lag in development at the apex relative to the base; numbers of cells, each from a different animal, are indicated next to the points. Measurements were made at −84 mV holding potential.

bundle deflections being larger than that for the normal polarity (Fig. 1*B*). In 70% of OHCs from *Lhfpl5*$^{-/-}$ mice (12 of 17 in which macroscopic currents were measured), a two-harmonic response was seen. No such two-harmonic response was seen in any *Lhfpl5*$^{+/-}$ heterozygotes [22 apical OHCs, postnatal day (P) P5–P6 mice]. Calibration of the bundle displacements evoked by the fluid-jet stimuli using high-speed imaging indicated comparable motion in the heterozygotes and knockouts and was used to derive current–displacement relationships in the two genotypes (Fig. S1). The component of two-harmonic current elicited by negative bundle deflection is reminiscent of that seen in *Tmc1/Tmc2* double mutants, or after tip-link destruction by prolonged exposure to 1,2-bis(o-aminophenoxy)ethane-N,N,N',N'-tetraacetic acid (BAPTA; 13, 18), or by mutations in tip-link cadherins (19), although in those instances, no residual normal polarity current was present. In the

Lhfpl5 knockouts, no significant variation in current amplitude from cochlear apex to base was found for either normal or reverse-polarity responses (Fig. 1 *C* and *D*).

Single-Channel Currents. Attenuation of the macroscopic current in the hair cells from *Lhfpl5*$^{-/-}$ mice is likely to be a composite effect of a reduction in the number of tip links and in the size of the single MT channel conductance. To parse out the contributions, single MT channels were assayed after isolation using brief BAPTA treatment to sever the majority of the tip links (15, 20). In the wild type, OHC single-channel conductances at the high-frequency base were about twofold larger than at the low-frequency apex, ranging from ~70 pS to 140 pS in 1.5 mM Ca^{2+} (Fig. 2 *A* and *C*) (12); OHC unitary conductances at both locations in vivo, where the bundle is exposed to low-Ca^{2+} endolymph, would be ~50% larger. In the *Lhfpl5*$^{-/-}$ mice, the OHC single-channel conductances for normal polarity stimuli were smaller at both cochlear locations, the reduction at the base being more marked than at the apex (Fig. 2 *B* and *D*). For most of the recordings, there was no indication of fast adaptation in the ensemble average responses, but this deficiency may be partly due to the large stimulus amplitudes used to characterize the channel currents (12). The tonotopic map of OHC single MT-channel conductances was determined for both wild-type and *Lhfpl5*$^{-/-}$ mice (Fig. 2*E*) and confirmed the larger reduction in channels in high-frequency OHCs. The gradient was diminished but not entirely lost in the mutant, similar to that seen for OHC channels in the *Tmc1*$^{-/-}$ mutant (12). To compare the effects in the *Tmc1* and *Lhfpl5* mutants, the ratio of mutant and control unitary currents in each case was plotted against cochlear location (Fig. 2*F*). This approach provided a better method of comparison because the absolute values in each mutant were slightly different, possibly because different genetic backgrounds were used. The ratio plots, although more extensive for the *Lhfpl5*$^{-/-}$, indicated that the quantitative reduction in OHC MT-channel conductance was similar for the two alleles.

Immunolabelling for TMC1 and LHFPL5. The apparent similarity of the MT ion channel properties in the *Lhfpl5* and the *Tmc1* mutants raises the possibility that one is linked to the other, a deficiency in LHFPL5 causing down-regulation or mislocalization of TMC1 or vice versa. Previous attempts to immunolabel for TMC1 with the normal fixation procedures have not been successful (9) so we used antigen retrieval methods, which in animals before the onset of hearing yielded diffuse TMC1 labelling in the bundle (Fig. 3*A*) as well as some in the cell body. Bundle structure was less well preserved due to the need to use organic solvents, but label for TMC1 was evident in the kinocilium (Fig. 3*A*), which is still present in the P5 animal. All labelling in both bundle and cell soma was absent in the *Tmc1Δ/Δ* mutant (Fig. 3*B*), confirming the specificity of the N-terminal antibody. Immunolabelling in cochleas of older, P12–P20, wild-type mice gave discrete labelling, more concentrated near the tops of the bundles (Fig. 3*D*); this more restricted localization could reflect the disappearance in more mature mice of the transient lateral links (21, 22), to which TMC1 might possibly be connected. Even in these older P16 mice, the resolution was insufficient to ascertain whether the TMC1 label occurred in all rows or was restricted only to the two shorter rows of stereocilia, as might be expected if it were connected to the MT channel (5). When cochleas from the *Lhfpl5*$^{-/-}$ mice were labelled with the anti-TMC1 antibody, no labelling was seen in the hair bundle (Fig. 3*C*). Similar results were obtained in five other animals. These observations raise the possibility that some or all of the effects of *Lhfpl5* mutation stem from a concomitant deficiency in TMC1. Complementary experiments, immunostaining for LHFPL5, were performed in *Tmc1/Tmc2* double mutants (Fig. S2). In the *Lhfpl5*$^{+/-}$ heterozygote, label occurred in discrete puncta toward the tips of the stereocilia (14). In the *Tmc1dn/dn Tmc2*$^{-/-}$
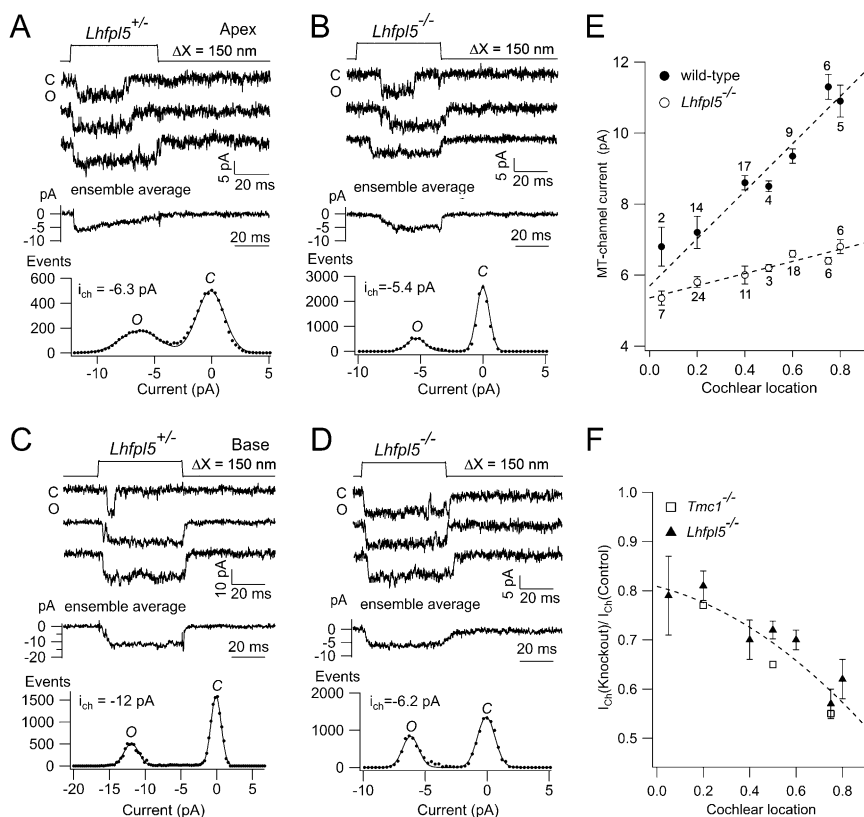
Fig. 2. Single MT channel currents in OHCs of *Lhfpl5* mutants. (*A–D*) Each panel shows three single MT channel currents for step displacements of bundle, an ensemble average, and an amplitude histogram. (*A*) *Lhfpl5*$^{+/-}$ heterozygote, cochlear apex; ensemble average of 18 responses, unitary current, −6.3 pA, P5 mouse; (*B*) *Lhfpl5*$^{-/-}$ knockout, cochlear apex; ensemble average of 10 responses, unitary current, −5.4 pA, P6 mouse; (*C*) *Lhfpl5*$^{+/-}$ heterozygote, cochlear base; ensemble average of 10 responses, unitary current, −12.0 pA, P3 mouse; and (*D*) *Lhfpl5*$^{-/-}$ knockout, cochlear base; ensemble average of 15 responses, unitary current, −6.2 pA, P2 mouse. (*E*) Collected results of MT current amplitudes (mean ± 1 SEM) as a function of cochlear location for wild-type and *Lhfpl5*$^{+/-}$ heterozygotes (combined results, filled circles), and *Lhfpl5*$^{-/-}$ knockouts (open circles). Number of cells averaged is given beside each point, each cell being from a different animal. All measurements were made at −84 mV holding potentials in 1.5 mM extracellular Ca^{2+} saline. (*F*) Ratio of single-channel current in *Lhfpl5*$^{-/-}$, I_{ch}(knockout), to single-channel current in control, I_{ch} (control), versus cochlear location, filled triangles (mean ± 1 SEM, from measurements in *E*). Open squares are results for *Tmc1* mutant, ratio of knockout to control, from ref. 12. Numbers of cells used to compute these ratios were (from apex to base) 9, 5, 9 (wild type), and 17, 3, 7 (*Tmc1*$^{-/-}$), each cell from a different animal.

mutant, the labelling appeared identical to that in the heterozygote, with particulate label near the tips of two rows of stereocilia in OHCs and one row in inner hair cells (IHCs). These results demonstrate that the LHFPL5 distribution, at least at the light microscopic level, is unaltered in the *Tmc1/Tmc2* double mutants.

Contribution of TMC2. If TMC1 is not targeted to the bundle in the *Lhfpl5*$^{-/-}$ mutant, what modulates the normal polarity (albeit reduced amplitude) MT current for the positive bundle displacements? In mice younger than P7, TMC2 is also present in the cochlea and has been proposed to substitute for TMC1 (9). Unlike in experiments with TMC1, we were unable to identify a specific antibody to immunolabel for TMC2. However, transfection with *Tmc2* gave spots of labelling in the stereocilia of *Lhfpl5*$^{+/-}$ heterozygotes (Fig. 4*A*), and targeting of TMC2 to the stereocilia persisted in *Lhfpl5*$^{-/-}$ (Fig. 4*B*), thus contrasting with the TMC1 results. To further assess the interaction, OHC MT currents were recorded in *Lhfpl5/Tmc2* double mutants (Fig. 4 *C* and *D*). When both genes were present as heterozygotes, large MT currents of normal polarity, elicited by bundle displacements toward the kinocilium, were observed. With *Lhfpl5*$^{-/-}$ *Tmc2*$^{+/-}$, a two-harmonic current was seen with an attenuated normal polarity response, similar to that in the single *Lhfpl5*$^{-/-}$ mice (Fig. 1*B*). However, when both *Tmc2* and *Lhfpl5* were knocked out, the normal-polarity MT current was much diminished

(mean = 27 ± 5 pA, in 7 *Lhfpl5*$^{-/-}$ *Tmc2*$^{-/-}$ hair cells in three animals) compared with the control current (1,010 ± 40 pA, five hair cells in three animals), leaving only the "reverse-polarity" component. Thus, even though a nonmutated *Tmc1* gene was present in the double mutant, its product did not support the MT current.

Interactions between the potential partners, LHFPL5, TMC1, and the tip-link protein PCDH15, were examined with immunoprecipitation experiments. PCDH15 occurs in three predominant isoform classes differing in their cytoplasmic domains: CD1, CD2, and CD3. The PCDH15-CD2 isoform is essential for the correct development of the cochlear hair bundles (23) and may be the major isoform in the tip link of adult auditory hair cells (24). Staining of HEK293 cells transfected to express PCDH15-CD2 and TMC1 revealed some colocalization of the two proteins, but most of the signal was in intracellular vesicles and not at the cell surface (Fig. S3). Both TMC1 and TMC2 coimmunoprecipitated with all three PCDH15 isoforms but not with control N-cadherin protein (Fig. 5*B*). This result is in agreement with recent studies (25) and suggests that all three PCDH15 isoforms can interact with TMC1 and TMC2. An interaction between TMC1 and PCDH15 could account for the TMC1 label in the kinocilium (Fig. 3), because PCDH15 is also present in the kinociliary links (26), as the CD2 isoform (23). In contrast, there was no evidence for coimmunoprecipitation of LHFPL5 by TMC1 (Fig. 5*A*).
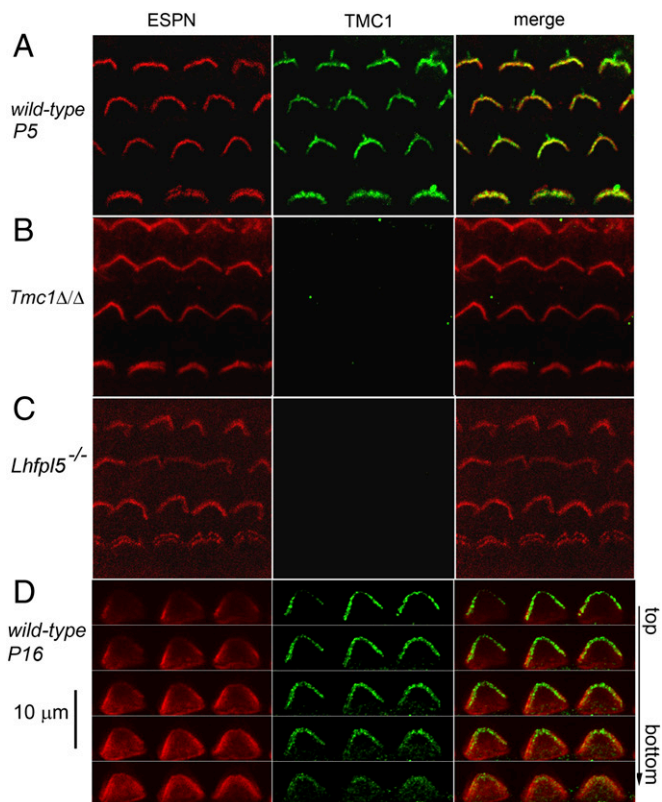
Fig. 3. Immunolabelling with anti-TMC1 antibody. (*A*) Surface preparation of apical cochlea of P5 wild type, showing three rows of OHC hair bundles (*Top*) and one row of IHC bundles (*Bottom*). (*Left*) ESPN labelling; (*Middle*) anti-TMC1 antibody; and (*Right*) merge. Note the bundles, including the OHC kinocilia, are labelled for TMC1. (*B*) Apical cochlea of P4 *Tmc1Δ/Δ* mutant, as in *A*. Note that there is no TMC1 antibody label in the knockout. (*C*) Apical cochlea of P5 *Lhfpl5*$^{-/-}$ mutant shows no TMC1 label in the bundles. The hair bundles in the *Lhfpl5*$^{-/-}$ mutant were more fragile and disorganized and the ESPN label was weaker, hence the higher background. Each image is an average of three 0.3-μm-thick stacks. (*D*) Apical cochlear OHCs of P16 wild type exhibited punctate TMC1 labelling toward the *Top* of the bundle, although the resolution was insufficient to determine whether labelling was present in all three stereociliary rows. The five traces are confocal sections from the *Top* to the *Bottom* of the bundles (~3 μm).

Discussion

We have documented MT channel properties of cochlear hair cells in *Lhfpl5* mutants, thereby extending previous findings, which demonstrated an interaction between LHFPL5 and protocadherin-15 at the lower end of the tip link (14). Our main conclusions are that in the *Lhfpl5*$^{-/-}$ mice (*i*) the macroscopic MT current in OHCs is reduced and it no longer varies tonotopically along the cochlea; (*ii*) single MT-channel currents follow a similar pattern of modification, with reduction in amplitude and diminution of the tonotopic gradient; and (*iii*) with reduction in the normal MT current, an abnormal mechanically sensitive current materializes, activated by the opposite (negative) polarity of hair bundle displacement.

The change in the macroscopic MT current in the *Lhfpl5*$^{-/-}$ mice is of composite origin, attributable to both reduction in single-channel conductance and loss of tip links (14). The relative contributions of the two processes can be inferred by comparing the ratio of knockout (I_{KO}) to control (I_C) macroscopic currents, ΔI ($= I_{KO}/I_C$; Fig. 1*C*) with the ratio of knockout (i_{KO}) to control (i_C) single-channel currents, Δi ($= i_{KO}/i_C$; Fig. 2*F*). Thus, at $d = 0.2$, the mean MT current is reduced from 710 pA to 207 pA, giving $\Delta I = 0.29$, whereas the single-channel ratio, Δi, is 0.8, indicating that the

fraction of tip links surviving is about one-third ($\Delta I/\Delta i = 36\%$). At $d = 0.8$, the mean MT current is reduced from 1,400 pA to 290 pA, giving $\Delta I = 0.21$, whereas the single-channel current ratio, Δi, is 0.6, indicating 35% survival of tip links. Thus, measurements at both locations indicate that ~35% of tip links persist in the mutant, a value that may be compared with direct measurements on scanning electron micrographs of hair bundles; counts of surviving tip links in *Lhfpl5*$^{-/-}$ mice gave values of 45% in OHCs and 36% in IHCs (14). These calculations confirm the prior conclusion that, even in the absence of LHFPL5, over a third of the tip links persist and are still able to activate MT channels. An important question with respect to the remaining tip links pertains to how force is transmitted from the protocadherin-15 to the MT channel: this might be achieved via TMC2 or another constituent such as transmembrane inner ear (TMIE) (27).

LHFPL5 is a tetraspan membrane protein analogous to the TARP proteins, which are allosteric regulators of AMPA receptor (28). Both LHFPL5 and TMC1 may be accessory (not pore forming) subunits and could fashion the external vestibule of the native channel (15, 29, 30); concentration of ions in this vestibule may be largely responsible for a single-channel conductance of large and variable size (6, 12). Because deficiency in either LHFPL5 or TMC1 had similar consequences, both proteins could
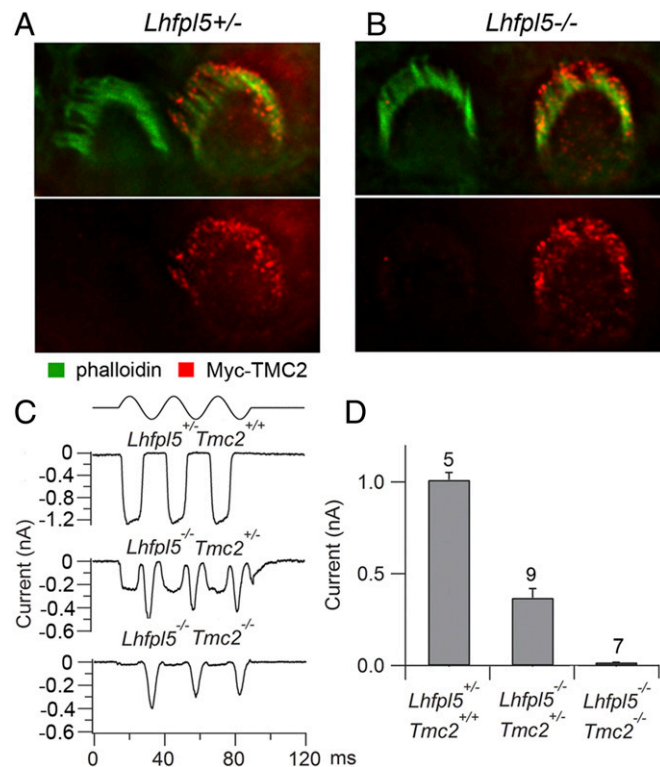
Fig. 4. Interaction between LHFPL5 and TMC2. (*A*) Apical OHCs of P4 *Lhfpl5*$^{+/-}$ heterozygote cochlea, transfected with *Tmc2*-Myc and cultured for 1 d in vitro and labelled with myc antibody (red) and phalloidin (green). (*B*) Apical OHCs of P4 *Lhfpl5*$^{-/-}$ homozygote cochlea, transfected with *Tmc2*-Myc, and cultured for 1 d in vitro and labelled as in *A*. TMC2 was still targeted to bundle despite the absence of LHFPL5. (*C*) MT currents for large (200 nm) bundle displacement in apical OHCs of *Lhfpl5*$^{+/-}$ *Tmc2*$^{+/+}$ (*Top*), *Lhfpl5*$^{-/-}$ *Tmc2*$^{+/-}$ (*Middle*), and *Lhfpl5*$^{-/-}$ *Tmc2*$^{-/-}$ (*Bottom*). (*D*) Collected MT currents (mean ± SEM) for the response component for positive displacement of hair bundle in the three mutants in *C*. The numbers of cells averaged are indicated next to the points, with recordings being collected from five *Lhfpl5*$^{+/-}$ *Tmc2*$^{+/+}$, six *Lhfpl5*$^{-/-}$ *Tmc2*$^{+/-}$, and three *Lhfpl5*$^{-/-}$ *Tmc2*$^{-/-}$ double knockout animals. The size of the reverse component was reduced from *Tmc2*$^{+/+}$ to *Tmc2*$^{+/-}$ to *Tmc2*$^{-/-}$.
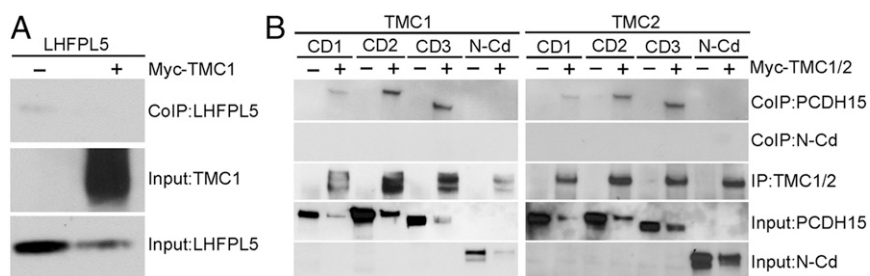
Fig. 5. Coimmunoprecipitations showing interactions between LHFPL5, TMC1, TMC2, and PCDH15. (*A*) HEK293 cells were transfected to express LHFPL5 either alone or together with Myc-TMC1. Immunoprecipitations were carried out with anti-Myc followed by Western blotting using anti-LHFPL5 for detection. The *Bottom* two lanes show input protein before immunoprecipitation. No protein interaction was in evidence. (*B*) HEK293 cells were transfected to express Myc-TMC1 or Myc-TMC2 alone, or together with PCDH15-CD1, -CD2, -CD3, or control GFP-tagged *N*-cadherin (*N*-Cd). Immunoprecipitations were carried out with anti-Myc followed by Western blotting with antibodies to the proteins indicated on the *Right*. The *Top* two panels show results from coimmunoprecipitations (Co-IP); the third row shows the amount of TMC1/2 proteins recovered in the immunoprecipitates (IP); the *Bottom* two rows show input PCDH15 and *N*-cadherin proteins in extracts before immunoprecipitation. Amounts of PCDH15 were consistently decreased by coexpressing TMC1 or TMC2, but coimmunoprecipitation was robustly observed.

be needed to stabilize the external vestibule. However, an alternative explanation is that loss of one protein leads to down-regulation of the other. This hypothesis was tested by labelling for each protein in *Lhfpl5* and *Tmc1* mutants, and it was demonstrated that loss of LHFPL5 down-regulated TMC1 but not vice versa; that is, LHFPL5 label and tip links were both present in *Tmc1* mutants. We propose therefore that the similarities in the effects of the *Tmc1* and *Lhfpl5* mutations, especially on the single-channel conductance, are mainly due to the absence of TMC1. TMC1 may be the principal accessory component forming the vestibule, and incorporation of variable amounts of TMC1 may account for gradation in the conductance along the cochlea (6). However, what determines the expression of TMC1? Is LHFPL5 needed as an obligatory chaperone, or is it the deficiency of PCHD15, and associated loss of tip links (as in the Ames waltzer mouse Pcdh15$^{av3J/av3J}$) (19), that can cause mislocalization of TMC1? Current evidence supports the model that PCDH15, TMC1, and LHFPL5 are part of a larger protein complex in the stereocilia. PCDH15 binds to LHFPL5 (14) and to TMC1 (25) (Fig. 5*B*). Interactions between TMC1 and LHFPL5 have so far not been detected, but LHFPL5 might stabilize the interaction between PCDH15 and TMC1. When TMC1 is absent, the tip links still develop (9, 13) and PCDH15 and LHFPL5 are still targeted to stereocilia (14). However, mutations of PCDH15 or LHFPL5 affect tip-link formation (14) and targeting of TMC1 to the stereocilia (Fig. 3).

Our present hypothesis is that the reverse-polarity current represents the pore-forming subunit of the native channel, but a number of important questions remain with regard to this current. For example, the location of the underlying channels is not precisely known, but they can be recruited under several conditions: (*i*) *Tmc1/Tmc2* double mutants (13); (*ii*) after tip-link loss either with BAPTA (13, 18) or in *av3J/av3J* and *v2J/v2J* mutations of *Pcdh15* and *Cdh23*, respectively (19); (*iii*) in *Lhfpl5*$^{−/−}$ mice; and (*iv*) in other mutants affecting bundle structure, including *Myo15 shaker 2* (31) and *Vlgr1* null (32). What connects these disparate processes and what might be the common signal to induce the channel response? Whereas the tip links are lost with BAPTA treatment, or in the *av3J/av3J* and *v2J/v2J* mutations (13, 19, 33), all links persist in the *Tmc1/Tmc2* double mutants (13), and a third remain in the *Lhfpl5*$^{−/−}$ mice (14). An alternative explanation is that loss of native MT channels leads to reduction in Ca^{2+} influx, which, by lowering the intracellular Ca^{2+} concentration, triggers the appearance of the reverse-polarity channels. More experiments are needed to address the significance and localization of these channels.

Materials and Methods

Mouse Mutants. MT currents were recorded from OHCs and IHCs in isolated organs of Corti of mice of either sex between 2 and 8 d postnatal (P2–P7, where P0 is the birth date) using methods previously documented (12–14, 34). Mutation in *Lhfpl5* (lipoma HMGIC fusion partner-like 5 gene, that causes human autosomal recessive hearing loss, DFNB67) (35, 36) was achieved with the B6.129-*Lhfpl5*^{tm1Kjn}/Kjn mouse strain (Jackson Labs; stock no. 005434), containing a targeted mutation in which exons 1 and 2 were replaced with a lacZ reporter cassette (14, 37). Controls were obtained with C57BL/6J or *Lhfpl*$^{+/−}$ heterozygotes. *Tmc1* gene mutations were obtained using *deafness* (CBA.Cg-*Tmc1*^{dn}/AjgJ; Jackson Labs), here referred to as *Tmc1dn/dn*; and one in which an IRES-lacZ cassette replaces exon 8 and exon 9 (ref 9; Jackson Labs (B6.129-*Tmc1*$^{tm1.1Ajg}$/J; stock no. 019146), here referred to as *Tmc1Δ/Δ*. The *Tmc2* mutation (B6.129S5-*Tmc2*^{tm1Lex}/Mmucd) was obtained from the Mutant Mouse Regional Resource Center, University of California, Davis, and as argued (12) is a knockout, being used to generate the double mutants *Tmc1dn/dn Tmc2*$^{−/−}$ and *Lhfpl5*$^{−/−}$*Tmc2*$^{−/−}$. Mice were genotyped from tail clips taken after dissection for the electrophysiology recordings and immunolabelling, in both cases the experimenter being blind to the genotype.

Electrophysiology and Stimulation. Mice were killed by decapitation using methods approved by the Institutional Animal Care and Use Committees of the University of Wisconsin-Madison and The Scripps Research Institute according to current National Institutes of Health guidelines. Excised cochlear turns were immobilized in a recording chamber mounted on a fixed-stage microscope (Leica DMFS) and viewed through a 63× water-immersion objective. Several cochlear locations were assayed, each designated by *d*, its distance along the basilar membrane from the apex normalized to the total length of the cochlea (~6.0 mm). The recording chamber was perfused with oxygenated saline of composition (in millimolar): 152 NaCl, 6 KCl, 1.5 CaCl$_2$, 2 Na-pyruvate, 8 D-glucose, and 10 Na-Hepes, pH 7.4, osmolarity ~315 mOsm/L, at room temperature, 21–23 °C. Electrical recordings were made with patch electrodes filled with (in millimolar): 128 CsCl, 3 0.5 MgCl$_2$, 5 Na$_2$ATP, 10 Tris phosphocreatine, 1 EGTA, 0.5 GTP, 0.5 cAMP, 10 Cs-Hepes, pH 7.2, ~295 mOsm/L, and connected to an Axopatch 200B amplifier with a 5-kHz output filter. Hair bundles were deflected with a fluid jet (11, 16), the stimulus usually being a 40-Hz sinusoid evoking a saturated current in wild type. Hair bundle motion elicited by a given voltage to the fluid jet piezoelectric disk was calibrated by high-speed imaging (Fig. S1). Single MT channels were isolated in whole-cell recordings by briefly exposing hair bundles to a saline with BAPTA-buffered submicromolar free 0.05 μM Ca^{2+} (13, 15). The validity of the measurements as representing single channels has been discussed (12) and justified by obtaining similar conductance values using an alternate procedure of channel block with the peptide GsMTx4 (12). Single-channel events were evoked by hair bundle deflections with a glass stylus driven by a calibrated piezoelectric stack actuator (15, 20). Unless otherwise stated, values are quoted as mean ± 1 SEM and statistical significance is assessed using a two-tailed Student's *t* test. Unless otherwise stated, each recording used to construct a mean was from a different animal.

Immunostaining. TMC1 was labelled in P5 mice with an antigen retrieval technique involving initial fixation in 4% (wt/vol) paraformaldehyde for 10 min

at room temperature, followed by secondary fixation and permeabilization in an equi-volume mixture of methanol and acetone at −20 °C for 10 min, followed by washing in PBS. For older (P14–P20) animals, temporal bones were fixed in 4% paraformaldehyde for 1 h at room temperature and, after overnight decalcification in 5% EDTA, dissected cochleas were permeabilized in 0.5% Triton for 30 min at room temperature and incubated in 10 mM Na citrate, pH 6.0, 75 °C for 30 min. All fixed cochleas were subsequently immersed in 10% normal goat serum (Invitrogen Life Sciences) for 1 h at room temperature and incubated overnight at 4 °C with the primary anti-TMC1 affinity-purified antibody (Sigma HPA 044166, made against a 39-residue N-terminal human TMC1 sequence) at a dilution of 1:50, 15 h (P5) or 1:200 for 30 h (P14–P20) followed by anti-rabbit Alexa Fluor-488 secondary antibody. Hair bundle morphology was revealed with a monoclonal anti-ESPN antibody (BD Bioscience; 1:100 dilution) or Alexa Fluor-568 phalloidin (1:200; Invitrogen Life Sciences). Mounted preparations were viewed with a 100× PlanApo objective (numerical aperture, 1.4) in a Nikon A1 laser-scanning confocal microscope. Each immunostaining run was performed on three cochleas from different animals, and this process was repeated three times, so nine animals in total were used for each labelling procedure.

Immunoprecipitation, Western Blot Analysis, and Transfection. Expression of murine Myc-TMC1, Myc-TMC2, PCDH15-CD1, PCDH15-CD2, PCDH15-CD3, LHFPL5, N-cadherin–EGFP constructs in HEK293 cells, immunoprecipitations, and Western blotting were carried out with methods described previously (14, 38). Primary antibodies were: anti-LHFPL5 (35); anti-PCDH15 PB811 (4); anti-Myc (Cell Signaling); and anti-GFP (14). Hair cells in cochlear cultures were transfected with Myc-Tmc2 containing plasmid using injectoporation (14, 39). Cochlear segments from P4 mice were cultured in DMEM/F12 medium with 1.5 mg/mL ampicillin, and the plasmid (1 µg/mL in HBSS) was delivered to the epithelium with a glass pipette. Regimes of three 60-V pulses, of 15-ms duration, were applied at 1-s intervals with an ECM 830 square wave electroporator. Cochleas were cultured for an additional day, fixed, and then labelled with anti-Myc antibody (Cell Signaling).

1. Pickles JO, Comis SD, Osborne MP (1984) Cross-links between stereocilia in the guinea pig organ of Corti, and their possible relation to sensory transduction. *Hear Res* 15(2):103–112.
2. Furness DN, Katori Y, Nirmal Kumar B, Hackney CM (2008) The dimensions and structural attachments of tip links in mammalian cochlear hair cells and the effects of exposure to different levels of extracellular calcium. *Neuroscience* 154(1):10–21.
3. Ahmed ZM, et al. (2006) The tip-link antigen, a protein associated with the transduction complex of sensory hair cells, is protocadherin-15. *J Neurosci* 26(26):7022–7034.
4. Kazmierczak P, et al. (2007) Cadherin 23 and protocadherin 15 interact to form tip-link filaments in sensory hair cells. *Nature* 449(7158):87–91.
5. Beurg M, Fettiplace R, Nam JH, Ricci AJ (2009) Localization of inner hair cell mechanotransducer channels using high-speed calcium imaging. *Nat Neurosci* 12(5):553–558.
6. Fettiplace R, Kim KX (2014) The physiology of mechanoelectrical transduction channels in hearing. *Physiol Rev* 94(3):951–986.
7. Kurima K, et al. (2002) Dominant and recessive deafness caused by mutations of a novel gene, TMC1, required for cochlear hair-cell function. *Nat Genet* 30(3):277–284.
8. Kurima K, Yang Y, Sorber K, Griffith AJ (2003) Characterization of the transmembrane channel-like (TMC) gene family: Functional clues from hearing loss and epidermodysplasia verruciformis. *Genomics* 82(3):300–308.
9. Kawashima Y, et al. (2011) Mechanotransduction in mouse inner ear hair cells requires transmembrane channel-like genes. *J Clin Invest* 121(12):4796–4809.
10. Pan B, et al. (2013) TMC1 and TMC2 are components of the mechanotransduction channel in hair cells of the mammalian inner ear. *Neuron* 79(3):504–515.
11. Kim KX, Fettiplace R (2013) Developmental changes in the cochlear hair cell mechanotransducer channel and their regulation by transmembrane channel-like proteins. *J Gen Physiol* 141(1):141–148.
12. Beurg M, Kim KX, Fettiplace R (2014) Conductance and block of hair-cell mechanotransducer channels in transmembrane channel-like protein mutants. *J Gen Physiol* 144(1):55–69.
13. Kim KX, et al. (2013) The role of transmembrane channel-like proteins in the operation of hair cell mechanotransducer channels. *J Gen Physiol* 142(5):493–505.
14. Xiong W, et al. (2012) TMHS is an integral component of the mechanotransduction machinery of cochlear hair cells. *Cell* 151(6):1283–95.
15. Beurg M, Evans MG, Hackney CM, Fettiplace R (2006) A large-conductance calcium-selective mechanotransducer channel in mammalian cochlear hair cells. *J Neurosci* 26(43):10992–11000.
16. Johnson SL, Beurg M, Marcotti W, Fettiplace R (2011) Prestin-driven cochlear amplification is not limited by the outer hair cell membrane time constant. *Neuron* 70(6):1143–1154.
17. Shotwell SL, Jacobs R, Hudspeth AJ (1981) Directional sensitivity of individual vertebrate hair cells to controlled deflection of their hair bundles. *Ann N Y Acad Sci* 374:1–10.
18. Marcotti W, et al. (2014) Transduction without tip links in cochlear hair cells is mediated by ion channels with permeation properties distinct from those of the mechano-electrical transducer channel. *J Neurosci* 34(16):5505–5514.
19. Alagramam KN, et al. (2011) Mutations in protocadherin 15 and cadherin 23 affect tip links and mechanotransduction in mammalian sensory hair cells. *PLoS ONE* 6(4):e19183.

20. Ricci AJ, Crawford AC, Fettiplace R (2003) Tonotopic variation in the conductance of the hair cell mechanotransducer channel. *Neuron* 40(5):983–990.
21. Goodyear RJ, Marcotti W, Kros CJ, Richardson GP (2005) Development and properties of stereociliary link types in hair cells of the mouse cochlea. *J Comp Neurol* 485(1):75–85.
22. Petit C, Richardson GP (2009) Linking genes underlying deafness to hair-bundle development and function. *Nat Neurosci* 12(6):703–710.
23. Webb SW, et al. (2011) Regulation of PCDH15 function in mechanosensory hair cells by alternative splicing of the cytoplasmic domain. *Development* 138(8):1607–1617.
24. Pepermans E, et al. (2014) The CD2 isoform of protocadherin-15 is an essential component of the tip-link complex in mature auditory hair cells. *EMBO Mol Med* 6(7):984–992.
25. Maeda R, et al. (2014) Tip-link protein protocadherin 15 interacts with transmembrane channel-like proteins TMC1 and TMC2. *Proc Natl Acad Sci USA* 111(35):12907–12912.
26. Goodyear RJ, Forge A, Legan PK, Richardson GP (2010) Asymmetric distribution of cadherin 23 and protocadherin 15 in the kinocilial links of avian sensory hair cells. *J Comp Neurol* 518(21):4288–4297.
27. Zhao B, et al. (2014) TMIE is an essential component of the mechanotransduction machinery of cochlear hair cells. *Neuron* 84(5):954–967.
28. Straub C, Tomita S (2012) The regulation of glutamate receptor trafficking and function by TARPs and other transmembrane auxiliary subunits. *Curr Opin Neurobiol* 22(3):488–495.
29. Farris HE, LeBlanc CL, Goswami J, Ricci AJ (2004) Probing the pore of the auditory hair cell mechanotransducer channel in turtle. *J Physiol* 558(Pt 3):769–792.
30. van Netten SM, Kros CJ (2007) Insights into the pore of the hair cell transducer channel from experiments with permeant blockers. *Curr Top Membr* 59:375–398.
31. Stepanyan R, Frolenkov GI (2009) Fast adaptation and Ca2+ sensitivity of the mechanotransducer require myosin-XVa in inner but not outer cochlear hair cells. *J Neurosci* 29(13):4023–4034.
32. Michalski N, et al. (2007) Molecular characterization of the ankle-link complex in cochlear hair cells and its role in the hair bundle functioning. *J Neurosci* 27(24):6478–6488.
33. Assad JA, Shepherd GM, Corey DP (1991) Tip-link integrity and mechanical transduction in vertebrate hair cells. *Neuron* 7(6):985–994.
34. Grillet N, et al. (2009) Harmonin mutations cause mechanotransduction defects in cochlear hair cells. *Neuron* 62(3):375–387.
35. Kalay E, et al. (2006) Mutations in the lipoma HMGIC fusion partner-like 5 (LHFPL5) gene cause autosomal recessive nonsyndromic hearing loss. *Hum Mutat* 27(7):633–639.
36. Shabbir MI, et al. (2006) Mutations of human TMHS cause recessively inherited non-syndromic hearing loss. *J Med Genet* 43(8):634–640.
37. Longo-Guess CM, Gagnon LH, Fritzsch B, Johnson KR (2007) Targeted knockout and lacZ reporter expression of the mouse Tmhs deafness gene and characterization of the hscy-2J mutation. *Mamm Genome* 18(9):646–656.
38. Senften M, et al. (2006) Physical and functional interaction between protocadherin 15 and myosin VIIa in mechanosensory hair cells. *J Neurosci* 26(7):2060–2071.
39. Xiong W, Wagner T, Yan L, Grillet N, Müller U (2014) Using injectoporation to deliver genes to mechanosensory hair cells. *Nat Protoc* 9(10):2438–2449.